Philosophical Magazine Letters
Publication details, including instructions for authors and subscription information:
http://www.tandfonline.com/loi/tphl20

Wavelike fracture pattern in a metallic glass: a Kelvin-Helmholtz flow instability

M.Q. Jiang[a][b], G. Wilde[b], C.B. Qu[c], F. Jiang[d], H.M. Xiao[c], J.H. Chen[a], S.Y. Fu[c] & L.H. Dai[a]

[a] State Key Laboratory of Nonlinear Mechanics, Institute of Mechanics, Chinese Academy of Sciences, Beijing 100190, China

[b] Institute of Materials Physics, Westfälische Wilhelms-Universität Münster, Münster 48149, Germany

[c] Technical Institute of Physics and Chemistry, Chinese Academy of Sciences, Beijing 100190, China

[d] State Key Laboratory for Mechanical Behavior of Materials, Xi'an Jiaotong University, Xi'an 710049, China

Published online: 08 Sep 2014.

To cite this article: M.Q. Jiang, G. Wilde, C.B. Qu, F. Jiang, H.M. Xiao, J.H. Chen, S.Y. Fu & L.H. Dai (2014) Wavelike fracture pattern in a metallic glass: a Kelvin-Helmholtz flow instability, Philosophical Magazine Letters, 94:10, 669-677, DOI: 10.1080/09500839.2014.955549

To link to this article: http://dx.doi.org/10.1080/09500839.2014.955549

Philosophical Magazine Letters, 2014
Vol. 94, No. 10, 669–677, http://dx.doi.org/10.1080/09500839.2014.955549

Wavelike fracture pattern in a metallic glass: a Kelvin–Helmholtz flow instability

M.Q. Jiang[a,b]*, G. Wilde[b], C.B. Qu[c], F. Jiang[d], H.M. Xiao[c], J.H. Chen[a], S.Y. Fu[c] and L.H. Dai[a]*

[a]*State Key Laboratory of Nonlinear Mechanics, Institute of Mechanics, Chinese Academy of Sciences, Beijing 100190, China;* [b]*Institute of Materials Physics, Westfälische Wilhelms-Universität Münster, Münster 48149, Germany;* [c]*Technical Institute of Physics and Chemistry, Chinese Academy of Sciences, Beijing 100190, China;* [d]*State Key Laboratory for Mechanical Behavior of Materials, Xi'an Jiaotong University, Xi'an 710049, China*

(*Received 24 March 2014; accepted 12 August 2014*)

We report a wavelike fracture pattern in a Zr-based bulk metallic glass that has been deformed under quasi-static uniaxial tensions between room temperature (300 K) and liquid nitrogen temperature (77 K). We attribute this wavelike pattern to a Kelvin–Helmholtz flow instability that occurs at certain interfaces between local cracking/softening regions. The instability criterion for the pattern formation is achieved via a hydrodynamic perturbation analysis, and furthermore, an instability map is built which demonstrates that the shear velocity difference on both sides of the interface is the main destabilizing factor. Finally, the characteristic instability time (the inverse of the instability growth rate) is explored by seeking the dispersion relation in the dominant (fastest) instability mode. The results increase the understanding of the flow and fracture of metallic glasses as well as the nature of their liquid structures.

Keywords: metallic glass; fracture pattern; Kelvin–Helmholtz instability

1. Introduction

One of the most striking features of a fluid is the ability to flow owing to a very limited resistance to shear. When a fluid is subjected to a significant shear, its flow is prone to be mechanically unstable into a turbulence where flow instabilities are frequently manifested by the emergence of waves or vortices [1–3]. Nevertheless, flow instabilities are not exclusive features of fluids, and actually can also take place in solids under the activation of sufficiently high energy. For example, confined sliding [4], high-speed impact [5] or nanosecond pulse laser [6] can induce the formation of (primitive) vortical structures in the plastic flow of crystalline metals, indicating the occurrence of flow instabilities. This situation is of paramount significance in relation to metallic glasses, since this type of disordered solids, in the popular and basically correct conception, is "frozen" liquids that have lost their ability to flow below the glass transition temperature [7–9]. In metallic glasses, a widely reported flow instability is the Saffman–Taylor (S–T) flow

*Corresponding authors. Email: mqjiang@imech.ac.cn (M.Q. Jiang); lhdai@lnm.imech.ac.cn (L.H. Dai)

instability, which describes that a crack (inviscid air) is pushed into a more viscous liquid layer (a shear band) driven by a negative pressure gradient [10,11]. The viscous fingering recently observed in nanosecond pulse laser ablation of a Zr-based bulk metallic glass also points towards an S-T flow instability [12]. Naturally, one would like to ask: are there any other types of flow instabilities that can take place in metallic glasses?

In the present work, we observed some wavelike configurations on the fracture surfaces of a typical Zr-based (Vitreloy 1) bulk metallic glass subjected to quasi-static uniaxial tensions over a wide range of temperatures. It is proposed that the wavelike fracture pattern results from a Kelvin–Helmholtz (K–H) flow instability that is governed by the competition between a shear velocity gradient and surface tension.

2. Experimental

A bulk metallic glass with nominal composition of $Zr_{41.2}Ti_{13.8}Cu_{12.5}Ni_{10.0}Be_{22.5}$ (Vitreloy 1) was chosen for this study because of its excellent glass-forming ability and high thermal stability compared with other systems [13,14]. Master alloy ingots were obtained by arc melting together the elements Zr, Ti, Cu, Ni and Be with a purity of 99.9% or better under a Ti-gettered Ar atmosphere. To ensure homogeneity, the master alloy ingots were re-melted several times and subsequently suction drawn into copper moulds to form plates ($100 \times 20 \times 2$mm). The glassy structure of as-cast plates was confirmed by X-ray diffraction in a Philips PW 1050 diffractometer using CuKα radiation.

Dogbone-like specimens, with gauge dimensions of $13 \times 2 \times 2$ mm^3 were obtained by lathe machining the as-cast Vitreloy 1 plates using a coolant. Uniaxial tension tests were performed with an Instron material testing machine under a strain rate of ~$10^{-4}\,s^{-1}$ at room temperature (300 K), 221 K, 152 K and liquid nitrogen temperature (77 K). At all temperatures, the Vitreloy 1 glass displays an elastic-brittle failure without appreciable macroscopical plasticity [15]. The fracture angles fall in the range of 55°–61°, demonstrating that the fracture is dominated by shear stress but affected by tensile normal stress [16–19]. After testing, an FEI Sirion scanning electron microscope was used to examine the fracture surfaces of all specimens.

3. Results

Figure 1a shows the representative fracture morphology of the Vitreloy 1 at 300 K. It is noted that the whole fracture surface consists of many sub-regions with different sizes. In each sub-region, there always exists a smooth core (marked by the arrows in Figure 1a) and radiating ridges of veins point to the core. It has been accepted that these smooth cores should be the nucleation sites of local sub-cracks within the shear band [17,20–22]. The shear band material can be considered as a viscous liquid [18,23–26], and the propagation of these local sub-cracks will further soften the shear band material ahead of them [27] and eventually lead to the final fracture. The vein ridges have been well explained by the S–T instability at the interface between the advancing sub-crack and the liquid layer ahead of the sub-crack tip [10,11]. At the moment of fracture, the propagating sub-cracks encounter each other, forming many interfaces. Quite interestingly, at some interfaces between the sub-regions, wavelike patterns on a microscale can

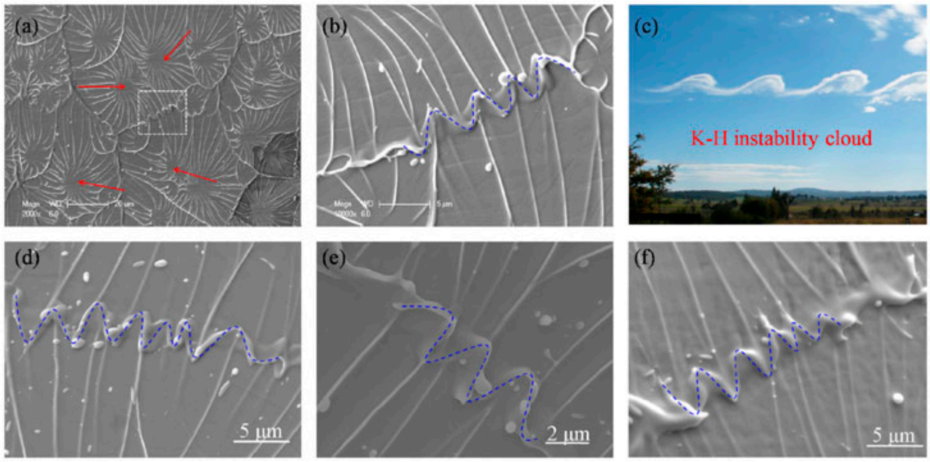

Figure 1. Microscale wavelike structures on tensile fracture surfaces of Vitreloy 1 metallic glasses at temperatures of 300 K (a and b), 221 K (d), 152 K (e) and 77 K (f). (b) is the magnified views of the rectangular area in (a). (c) Similarly shaped K–H instability cloud (Ref. [29]) on a scale 10^8 times that of (b, d–f).

be observed, as shown in Figure 1b, which displays an enlarged view of the rectangular area in Figure 1a. This kind of interface configuration directs our attention to the K–H instability in hydrodynamics [28]. For instance, Figure 1c shows a typical K–H instability case [29], a "billow cloud" that is very rare and exceptional but can be seen on some days. The K–H instability cloud is the result of an interface instability between the cloud and the wind caused by a strong relative shear. The wavelike fracture pattern in Figure 1b is very similar to the billow cloud in Figure 1c, although their scales are different by at least eight orders of magnitude.

More importantly, the wavelike configurations can also be observed in samples strained at other temperature: 221, 152 and 77 K, as displayed in Figures 1d–f, respectively. It is noticed that the characteristic wavelength (about 1–5 μm) of these configurations is not greatly affected by the temperature change, which implies that their formation is mainly determined by flow dynamics (or the inertia). The temperature independence of fracture patterns is also consistent with the fact that shear bands in front of the sub-cracks are in the flow state with a saturation concentration of the free volume [30].

4. Theoretical analysis and discussion

Clearly, the observed wavelike pattern at the interface results from the interplay of local sub-cracks. Without loss of generality, we consider two nucleation sites, N_1 and N_2, of local sub-cracks on the main fracture surface that is localized in an Eulerian coordinate system (x, y), as illustrated in Figure 2. Once nucleated in the dominated shear band, the two sub-cracks begin to advance with velocities of $\mathbf{v}_1$ and $\mathbf{v}_2$, respectively. The advancing sub-crack pushes the liquid layer ahead of the crack tip with the same velocity. The propagation of the sub-cracks should inevitably lead to a relative shear motion of two liquids in the vicinity of their interface that is assumed to be at $y = 0$.

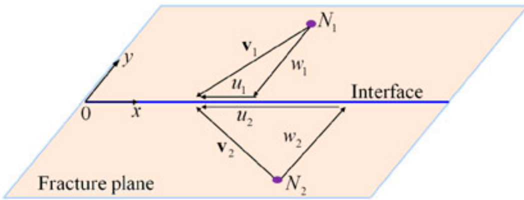

Figure 2. Schematics of the interplay of two sub-cracks nucleated at the sites N_1 and N_2, respectively, on the main fracture plane modelled in an Eulerian coordinate system (x, y). The two sub-cracks propagate with the velocities of $\mathbf{v}_1$ and $\mathbf{v}_2$, respectively.

Evidence for the shear motion at the interfaces is from the observation that radiating ridges of veins caused by the S–T instability is not strictly perpendicular to the interfaces (see Figure 1). This leads to a difference in the velocities of two neighbouring liquids projected on to their interface. It is reasonable to believe that this relative shear motion of the two liquids induces the K–H flow instability that manifests in the form of a wavelike interface. Here, we assume the two liquids with saturated free volume as Newtonian fluids [30–33] and incompressible, and the effect of surface tension between them is taken into account. Considering the characteristic length is at micrometre scales, the surface tension is assumed to be a constant [34]. The hydrodynamic equations for the two fluids and their interface can be written as:

$$\rho D_t u + \partial_x p - \mu \Delta u = 0, \tag{1}$$

$$\rho D_t w + \partial_x p - \mu \Delta w = \sigma \frac{\partial^2 y_s}{\partial x^2} \delta(y - y_{s0}), \tag{2}$$

$$D_t \rho = 0, \tag{3}$$

$$\nabla \cdot \mathbf{v} = 0, \tag{4}$$

$$D_t y_s = w_s, \tag{5}$$

where (1) and (2) are the conservation laws for momentum along the x-direction and y-direction, respectively, (3) the incompressibility condition, (4) the continuity equation and (5) the interface continuity condition. In these equations, $D_t \equiv \partial_t + \mathbf{v} \cdot \nabla$ is the material derivation, ρ is the density, u and w are the components of $\mathbf{v}$ along the x-direction and y-direction, respectively; μ denotes the coefficient of viscosity, p is the pressure, σ is the surface tension constant, δ is the Dirac delta function, the subscript "s" denotes the interface and $y_{s0} = 0$ is the initial position of the interface.

We consider a small deviation $y'_s$of the initial interface (y_{s0}) with the form $\exp i(\omega t + kx)$. This perturbation will cause small deviations $\{u', w', p', \rho', \mu'\}$ of other hydrodynamic variables $\{u_0, w_0, p_0, \rho_0, \mu_0\}$ with an identical form. It is, therefore, interesting to concentrate on the evolution of the disturbed interface. In order to highlight the essential physics, we assume that $u_0 = u_0(y)$, $w_0 = \text{const.}1$, $\rho_0 = \rho_0(y)$ and $\mu_0 = \text{const. } 2$. These assumptions are consistent with the common consideration for the steady-state homogeneous flow in a shear band [30,35–37]. Here, k is the wave number related to the spatial scale of the instability and $\omega = \gamma + i\alpha$, here, α is the growth rate of the instability. The stability of the interface is actually determined by the sign of α. If $\alpha \geq 0$, it is stable, otherwise, unstable.

Inserting the perturbations into Equations (1)–(5) and only retaining the first-order terms of the perturbed velocity w', we can derive the governing equation for the perturbed state:

$$\begin{aligned}&-i\rho_0(\omega+ku_0)\left(\Gamma^2-k^2\right)w'+\mu_0\left(\Gamma^2-k^2\right)\Gamma^2w'-\mu_0\left(\Gamma^2-k^2\right)k^2w'\\&\quad-i\Gamma\rho_0(\omega+ku_0)\Gamma w'-ik\rho_0\Gamma u_0\Gamma w'+ik\Gamma\rho_0\Gamma u_0w'+ik\rho_0\Gamma^2u_0w'+ik\rho_0\Gamma u_0\Gamma w'\\&\quad-ik\Gamma\mu'\Gamma^2u_0-ik\mu'\Gamma^3u_0\\&\quad=-\sigma k^4y'\delta(y),\end{aligned} \tag{6}$$

where $\Gamma = \partial_y$. Through the integral approximation, the interface condition that is satisfied at a surface of the discontinuity can be given by:

$$\begin{aligned}&\Delta_s\left[-\rho_0i(\omega+ku_0)\Gamma w'+i\rho_0k\Gamma u_0w'+\mu_0\left(\Gamma^2-k^2\right)\Gamma w'-i\mu'k\Gamma^2u_0-\mu_0k^2\Gamma w'\right]\\&\quad=-\sigma k^4y'_s,\end{aligned} \tag{7}$$

where $\Delta_s = f_{y_{s0}+0} - f_{y_{s0}-0}$. It should be kept in mind that the domain of interest is the two thin fluid layers in the vicinity of the interface. Thus, we shall further suppose that the two fluids are flowing with the constant velocities u_{01} and u_{02} as well as at constant densities ρ_{01} and ρ_{02}. We can immediately obtain the solution of Eq. (6) except for the interface, that is

$$w'_n = y'_s i(\omega + ku_{01})e^{(-1)^n ky} \quad (n = 1, 2). \tag{8}$$

Applying the solution to the interface condition (7) yields the spectral equation for the growth rate α of the perturbation:

$$a_4\alpha^4 + a_3\alpha^3 + a_2\alpha^2 + a_1\alpha + a_0 = 0, \tag{9}$$

with

$$a_4 = 4(\rho_{01} + \rho_{02})^3, \tag{10a}$$

$$a_3 = -8k^2(\mu_{01} + \mu_{02})(\rho_{01} + \rho_{02})^2, \tag{10b}$$

$$a_2 = k(\rho_{01} + \rho_{02})[5k^3(\mu_{01} + \mu_{02})^2 + 4k^2\sigma(\rho_{01} + \rho_{02}) - 4k\rho_{01}\rho_{02}(u_{01} - u_{02})^2], \tag{10c}$$

$$a_1 = -k^3(\mu_{01} + \mu_{02})[k^3(\mu_{01} + \mu_{02})^2 + 4k^2\sigma(\rho_{01} + \rho_{02}) - 4k\rho_{01}\rho_{02}(u_{01} - u_{02})^2], \tag{10d}$$

$$a_0 = k^7\sigma(\mu_{01} + \mu_{02})^2 - k^6(u_{01} - u_{02})^2\left(\rho_{01}\mu_{02}^2 + \rho_{02}\mu_{01}^2\right) \tag{10e}$$

According to the Routh-Hurwitz criterion [38], the instability criterion for the interface can be obtained as:

$$|u_{01} - u_{02}| > (\mu_{01} + \mu_{02})\sqrt{\frac{\sigma k}{\rho_{01}\mu_{02}^2 + \rho_{02}\mu_{01}^2}}. \tag{11}$$

This criterion indicates that the difference in initial horizontal velocity $\Delta u_0 = |u_{01} - u_{02}|$ incurs the interface instability, whereas the surface tension σ suppresses the instability development. Obviously, the fluid viscosity (μ_{01} and μ_{02}) also affects the interface stability. In physics, this kind of configuration just satisfies the K–H instability [28].

Based on the instability criterion (11), the dynamic balance between the stabilizing and destabilizing effects determines a critical wavelength:

$$\lambda_c = \frac{2\pi(\mu_{01} + \mu_{02})^2}{\rho_{01}\mu_{02}^2 + \rho_{02}\mu_{01}^2} \frac{\sigma}{\Delta u_0^2}. \tag{12}$$

The critical wavelength, from a viewpoint of the spatial scale, determines whether a perturbation will grow unstably or die out. Perturbations with a wavelength smaller than λ_c will disappear, whereas the ones with a wavelength larger than λ_c will lead to a run-away instability. Equation (12) shows that the critical instability wavelength depends not only on the material parameters (ρ_0, μ_0 and σ) but also on the relative shear velocity Δu_0 of the two fluids. According to our previous work [39], the crack propagation velocity of the Vitreloy 1 is about 1–2% of the Rayleigh wave speed (about 2200 ms^{-1}) at the vein-pattern stage. Thus, an interval $0 \leq \Delta u_0 \leq 80\ \mathrm{ms}^{-1}$is reasonably obtained. Further, we neglect the trivial difference in density and viscosity of the two fluids. We plot the critical instability wavelength versus the relative shear velocity for the surface tension $\sigma \approx 0.83\ \mathrm{Nm}^{-1}$ [40], which constructs an instability map (see Figure 3). The map predicts that the critical instability wavelength decreases with increasing Δu_0, which separates the domain into an unstable (upper) and a stable (lower) one. Higher Δu_0 will make the instability take place more easily. At the limit $\Delta u_0 \to 0$, it predicts $\lambda_c \to \infty$, which means a stable state. For the present experiments, the characteristic wavelength of the wavelike patterns is about 1–5 μm (Figure 1) that is marked by two dashed lines in the instability map (Figure 3). According to the map,

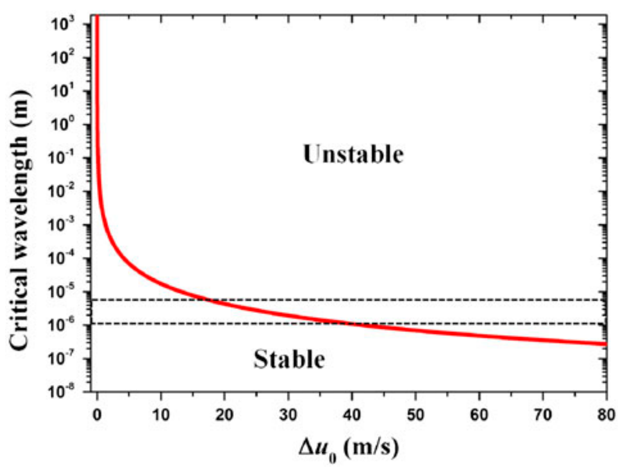

Figure 3. An instability map constructed by the plot of the critical instability wavelength as a function of the relative shear velocity of two viscous fluids.

the relative shear velocity of the two fluids should be larger than a critical value (about 20 ms^{-1}) to guarantee the occurrence of the K–H instability. The result explains why the wavelike pattern can be only observed at certain interfaces that just satisfy the K–H instability condition, i.e. Equations (11) or (12), instead of observing it at all interfaces. It in turn provides the evidence that only at the wavelike interfaces, there exists the strong shear motion of liquids. The good agreement between the predicted critical wavelength and the measured wavelength validates that the K–H instability is a candidate mechanism for the observed wavelike fracture patterns.

It is also interesting to examine the characteristic instability time to see if there is a sufficient time to allow the K–H instability to occur. The characteristic instability time is the inverse of the absolute value of the instability growth rate in the dominant (fastest) mode that is determined by the dispersion relation $\partial\alpha_m/\partial k_m = 0$. We plotted it for $\Delta u_0 \geq 20\ ms^{-1}$ in Figure 4. It can be seen that for each Δu_0 the instability growth rate increases with increasing wave number. This means that the smaller the instability wavelength, the faster the instability takes place. Furthermore, for a fixed wave number (or instability wavelength), a higher Δu_0 will increase the instability growth rate, also leading to a faster instability. According to our current observations, the characteristic wavelength (about 1–5 μm) of the wavelike patterns corresponds to the range $1.26 \times 10^6\ m^{-1} \leq k \leq 6.28 \times 10^6\ m^{-1}$ indicated by the double-headed arrow in Figure 4. In this range of wave numbers, the characteristic instability time ranges from microseconds to tens of microseconds which is less than the characteristic time of shear banding (inhomogeneous flow) propagation [41,42]. This ensures that the K–H instability has sufficient time to occur during inhomogeneous flow in front of moving cracks. However, it is noted that the observed wavelike configurations induced by the K–H instability do not develop into mature vortices. The reason is maybe related to the highly dissipative nature of metal plasticity and the greater resistance to flow, which prevents the further development of the wavelike structures and confines them to the early stage of the onset of turbulence.

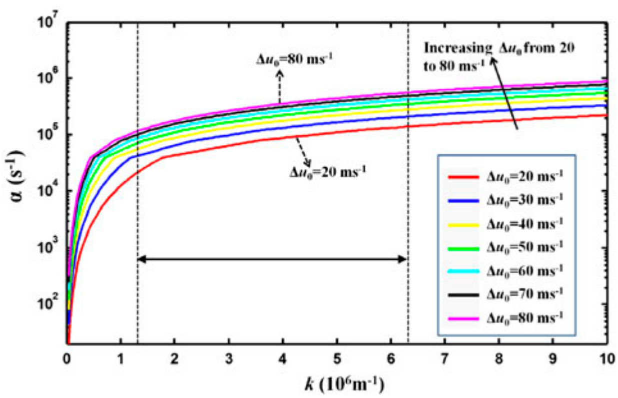

Figure 4. The dispersion relations in the dominant instability mode at different relative shear velocities. The region marked by the arrow corresponds to the current observation.

5. Conclusions

Quasi-static uniaxial tensile experiments were performed on Vitreloy 1 bulk metallic glasses between room temperature and liquid nitrogen temperature. In this temperature range, wavelike patterns are observed on the facture surfaces. It is proposed that this wavelike fracture pattern results from the K–H flow instability of fluids at sub-crack tips. Based on a hydrodynamic instability analysis, such mechanism is highlighted by exploring the critical instability wavelength and the characteristic instability time. We believe that wavelike flow patterns could be observed in other situations of metallic glasses [43], so long as the underlying K–H instability mechanism becomes activated. Finally, it must be pointed out that the compressive stress on the shear plane usually restrains the free volume creation [44] or cavitation [15,18], and the resulting nucleation of local sub-cracks. We, therefore, expect that the wavelike fracture pattern can be rarely observed in metallic glasses under uniaxial compressions.

Acknowledgements

M.Q.J. gratefully acknowledges the Alexander von Humboldt Foundation for the support with a research fellowship. G.W. acknowledges the support by DFG. L.H.D. acknowledges the CAS/SAFEA International Partnership Program for Creative Research Teams.

Funding

Financial support is from the NSFC [grants number 11372315], [grants number 11132011], [grants number 11023001], [grants number 51171138] and the National Key Research Program of China [grants number 2012CB937500].

References

[1] H.J. Lugt, *Vortex Flow in Nature and Technology*, John Wiley, New York, 1983.
[2] D.J. Evans and G.P. Morriss, Phys. Rev. Lett. 56 (1986) p.2172.
[3] B.J. Rosenberg, M. Hultmark, M. Vallikivi, S.C.C. Bailey and A.J. Smits, J. Fluid Mech. 731 (2013) p.46.
[4] N.K. Sundaram, Y. Guo and S. Chandrasekar, Phys. Rev. Lett. 109 (2012) p.106001.
[5] P.R. Guduru, G. Ravichandran and A.J. Rosakis, Phys. Rev. E 64 (2001) p.036128.
[6] S. Lugomer, Phys. Lett. A 361 (2007) p.87.
[7] A.L. Greer, Science 267 (1995) p.1947.
[8] P.G. Debenedetti and F.H. Stillinger, Nature 410 (2001) p.259.
[9] M.W. Chen, NPG Asia Mater. 3 (2011) p.82.
[10] P.G. Saffman and G. Taylor, Proc. R. Soc. London, A 245 (1958) p.312.
[11] A.S. Argon and M.S. Salama, Mater. Sci. Eng. 23 (1976) p.219.
[12] Y. Liu, M.Q. Jiang, G.W. Yang, J.H. Chen, Y.J. Guan and L.H. Dai, Intermetallics 31 (2012) p.325.
[13] A. Peker and W.L. Johnson, Appl. Phys. Lett. 63 (1993) p.2342.
[14] W.L. Johnson, MRS Bull. 24 (1999) p.42.
[15] M.Q. Jiang, G. Wilde, J.H. Chen, C.B. Qu, S.Y. Fu, F. Jiang and L.H. Dai, Acta Mater. 77 (2014) p.248.
[16] J.J. Lewandowski and P. Lowhaphandu, Philos. Mag. A 82 (2002) p.3427.
[17] Z.F. Zhang, J. Eckert and L. Schultz, Acta Mater. 51 (2003) p.1167.

[18] M.Q. Jiang, Z. Ling, J.X. Meng and L.H. Dai, Philos. Mag. 88 (2008) p.407.
[19] Y. Chen, M.Q. Jiang, Y.J. Wei and L.H. Dai, Philos. Mag. 91 (2011) p.4536.
[20] H.J. Leamy, T.T. Wang and H.S. Chen, Metall. Trans. A 3 (1972) p.699.
[21] C.A. Pampillo, J. Mater. Sci. 10 (1975) p.1194.
[22] R.T. Qu, M. Stoica, J. Eckert and Z.F. Zhang, J. Appl. Phys. 108 (2010) p.063509.
[23] D. Klaumünzer, A. Lazarev, R. Maaß, F.H. Dalla Torre, A. Vinogradov and J.F. Löffler, Phys. Rev. Lett. 107 (2011) p.185502.
[24] J. Bokeloh, S.V. Divinski, G. Reglitz and G. Wilde, Phys. Rev. Lett. 107 (2012) p.235503.
[25] R. Maaß, D. Klaumünzer, G. Villard, P.M. Derlet and J.F. Löffler, Appl. Phys. Lett. 100 (2012) p.071904.
[26] G. Wang, D.Q. Zhao, H.Y. Bai, M.X. Pan, A.L. Xia, B.S. Han, X.K. Xi, Y. Wu and W.H. Wang, Phys. Rev. Lett. 98 (2007) p.235501.
[27] H.W. Zhang, G. Subhash and S. Maiti, J. Appl. Phys. 102 (2007) p.043519.
[28] S. Chandrasekhar, *Hydrodynamic and hydromagnetic stability*, Dover, New York, 1981.
[29] http://en.wikipedia.org/wiki/File:Wavecloudsduval.jpg
[30] F. Spaepen, Acta Metall. 25 (1977) p.407.
[31] A. Furukawa and H. Tanaka, Nat. Mater. 8 (2009) p.601.
[32] N. Li, Y. Chen, M.Q. Jiang, D.J. Li, J.J. He, Y. Wu and L. Liu, Acta Mater. 61 (2013) p.1921.
[33] C.A. Schuh, T.C. Hufnagel and U. Ramamurty, Acta Mater. 55 (2007) p.4067.
[34] P. Guan, S. Lu, M.J.B. Spector, P.K. Valavala and M.L. Falk, Phys. Rev. Lett. 110 (2013) p.185502.
[35] A.S. Argon, Acta Metall. 27 (1979) p.47.
[36] M.Q. Jiang and L.H. Dai, J. Mech. Phys. Solids 57 (2009) p.1267.
[37] M.Q. Jiang, W.H. Wang and L.H. Dai, Scr. Mater. 60 (2009) p.1004.
[38] D.A. Sanchez, *Ordinary differential equations and stability theory*, Freeman, San Francisco, CA, 1968.
[39] J.X. Meng, Z. Ling, M.Q. Jiang, H.S. Zhang and L.H. Dai, Appl. Phys. Lett. 92 (2008) p.171909.
[40] W.J. Wright, T.C. Hufnagel and W.D. Nix, J. Appl. Phys. 93 (2003) p.1432.
[41] D. Klaumünzer, R. Maaß and F.H. Dalla Torre and J.F. Löffler, Appl. Phys. Lett. 96 (2010) p.061901.
[42] R. Maaβ, D. Klaumünzer and J.F. Löffler, Acta Mater. 59 (2011) p.3205.
[43] A.R. Yavari, K. Georgarakis, W.J. Botta, A. Inoue and G. Vaughan, Phys. Rev. B 82 (2010) p.172202.
[44] K.M. Flores and R.H. Dauskardt, Acta Mater. 49 (2001) p.2527.